Combining Ceftriaxone with Doxycycline and Daptomycin Reduces Mortality, Neuroinflammation, Brain Damage and Hearing Loss in Infant Rat Pneumococcal Meningitis

Running title: Triple Antibiotic Therapy in Pneumococcal Meningitis

Lukas Muri[1,2], Michael Perny[1], Jonas Zemp[1], Denis Grandgirard[1] and Stephen L. Leib[1,#]

[1] Neuroinfection Laboratory, Institute for Infectious Diseases, University of Bern, Friedbühlstrasse 51, 3001 Bern

[2] Graduate School for Cellular and Biomedical Sciences (GCB), University of Bern, Freiestrasse 1, 3012 Bern

[#] Corresponding author: Stephen.leib@ifik.unibe.ch

Corresponding author:

Stephen L. Leib
stephen.leib@ifik.unibe.ch
Institute for Infectious Diseases
University of Bern
Friedbühlstrasse 51
3001 Bern
Switzerland

E-mail addresses:

lukas.muri@ifik.unibe.ch
michael_perny@yahoo.de
jonas.1313@hotmail.com
denis.grandgirard@ifik.unibe.ch
stephen.leib@ifik.unibe.ch

Abstract

Despite available antibiotic therapy, pneumococcal meningitis (PM) is associated with a case fatality rate of up to 30% in high-income countries. Survivors often suffer from severe lifelong disabilities. An excessive inflammatory reaction drives the pathophysiology leading to brain damage and neurologic sequelae. We aimed to improve the outcome of experimental PM by simultaneously targeting different pathophysiological mechanisms with combined adjunctive therapies previously shown to be neuroprotective. *In vitro*, the anti-inflammatory effect of doxycycline and daptomycin were evaluated on primary rat astroglial cells stimulated with *S. pneumoniae*. Eleven day old infant Wistar rats were infected intracisternally with *S. pneumoniae* and randomized for treatment with ceftriaxone or combination adjuvant therapy consisting of ceftriaxone, daptomycin and doxycycline. During acute PM, combined adjuvant therapy with ceftriaxone, daptomycin and doxycycline increased survival rate from 64.1% to 85.8% ($p<0.01$) and alleviated weight loss compared to ceftriaxone monotherapy ($p<0.01$). Levels of inflammatory cytokines were significantly reduced by combined adjuvant therapy *in vitro* ($p<0.0001$) and in cerebrospinal fluid *in vivo* ($p<0.05$). In infected animals treated with combined adjunctive therapy, cortical damage was significantly reduced ($p<0.05$) and they showed a trend towards better hearing capacity three weeks after the infection ($p=0.089$), an effect which was significant in mildly infected animals (48dB vs 67.22dB, $p<0.05$). These mildly infected animals showed significantly reduced cochlear fibrous occlusion ($p<0.01$). By combining non-bacteriolytic daptomycin and anti-inflammatory doxycycline with ceftriaxone, their previously reported beneficial effects were cumulated and identified the triple antibiotic therapy as a promising therapeutic option for paediatric PM.

Key words

Pneumococcal meningitis, brain injury, neurologic sequelae, neuroinflammation, hearing loss, combination adjuvant therapy

Introduction

Acute bacterial meningitis is a severe illness with high mortality and morbidity – especially when acquired during infancy or childhood – causing long-lasting neurofunctional deficits (e.g. hearing loss, epilepsy, cerebral palsy and cognitive deficits), which tremendously influence quality of life in affected children (1–6). Currently, *Neisseria meningitidis* and *Streptococcus pneumoniae* are the most prevalent etiological agents for childhood meningitis beyond the neonatal age, as *Haemophilus influenza* type b has been nearly eradicated since vaccine introduction (7). In high-income countries, meningitis caused by *S. pneumoniae* and *N. meningitidis* presents case-fatality rates of 30% and 7%, respectively (6, 8). Fatality rates are reported to be as high as 50% in resource-poor setting (9). The risk for neurologic sequelae is especially high after pneumococcal meningitis (PM) (3), which causes a massive infection of the central nervous system (CNS) with associated cortical necrosis and apoptosis of dentate gyrus granular cells progenitors in the hippocampus, as found in human patients (10) and animal models (11–14). Neural cell death is caused by multiple factors including bacterial toxins and an excessive inflammatory reaction from the host (15–17). Together with the recruited neutrophils, activated brain-resident microglia are able to produce large quantities of inflammatory cytokines, reactive oxygen and nitrogen species (ROS and RNS), helping to eradicate the pathogen but also contributing to the development of neuronal damage (15, 18, 19). Pathological cell death in the hippocampus during acute PM correlates with learning and memory deficits (20–23). Furthermore, PM induces damage in the peripheral nervous system (PNS) characterised by sensorineural hearing loss caused by damage to hairs cells and spiral ganglion neurons in the inner ear (24–26), provoking hearing impairments in up to 30% of survivors (3, 4, 6).

Clinical guidelines recommend the use of adjunctive dexamethasone – an anti-inflammatory corticosteroid – for adult PM in high income countries (27, 28). However, adjuvant dexamethasone failed to provide a beneficial effect on PM-induced mortality and hearing loss in children (27, 29) and even aggravated mortality, acute brain injury and long-term learning deficits in different experimental models of bacterial meningitis (23, 30, 31). Over the last few decades, alternative adjuvant therapies including antioxidants, complement inhibitors, non-bacteriolytic antibiotics or matrix

metalloproteinase (MMP) inhibitors, which target different pathophysiological mechanisms during acute PM were tested and have shown promising results in PM animal models (32–39). These therapies were mostly evaluated as single adjuvant therapies or in combination with dexamethasone (40, 41), being less relevant in paediatric meningitis. We recently postulated to combine successful single adjuvants to more effectively reduce CNS and PNS damage thereby improving long-term outcome by reducing neurologic sequelae after paediatric PM. This strategy was successfully tested in the same experimental model as described in this present study by combining daptomycin (DAP) and the matrix metalloproteinase inhibitor Trocade (42). An independent experimental study also reported beneficial effects of combining adjuvant therapies to improve acute and neurofunctional outcomes after murine PM (43).

DAP has previously been shown to clear pneumococci from CSF more rapidly than ceftriaxone (CRO) without inducing bacterial lysis, thereby lowering the overall inflammatory burden in animal models (44, 45). DAP penetrates into the CSF – especially after neurological infection (46, 47) – and reaches 5-11.5% of serum concentration mediating bactericidal effects (46–48). In infant rat PM, adjunctive daptomycin reduced neuroinflammatory cytokines in the cerebrospinal fluid (CSF) and decreased brain injury and hearing loss (32, 42). Apart from its antimicrobial activity, doxycycline (DOX) – which is known to penetrate well into the brain and CSF (49) – also has multiple anti-inflammatory effects by reducing cytokine release and inhibiting MMP activity (50–56). Adjuvant DOX reduced mortality and injury to the brain and cochlea in experimental infant rat PM (56), similarly to other MMP inhibitors that were shown to reduce blood-brain barrier permeability, inflammatory cytokines in CSF, brain injury and mortality during acute bacterial meningitis (34, 42, 57, 58).

By combining adjunctive DAP and DOX therapies, we intend to target multiple pathophysiological mechanisms responsible for brain injury during acute bacterial meningitis with the aim to integrate the beneficial effects of both substances and improve the neurofunctional outcome after paediatric PM.

Results

Antibiotic susceptibility of S. pneumoniae serotype 3

The MIC of ceftriaxone for the used *S. pneumoniae* serotype 3 was determined to be 0.003mg/L. MICs of daptomycin and doxycycline were both at 0.064mg/L. Determined MICs revealed susceptibility of our *S. pneumoniae* serotype 3 strain to assessed antibiotics according to published data (59, 60).

Reduced release of inflammatory cytokines and nitric oxide *in vitro*

Inflammatory cytokines and nitric oxide (NO) were measured in astroglial cell culture supernatant 24 hours after concomitant application of living *S. pneumoniae* and antibiotics. Antibacterial but bacteriolytic therapy with CRO induced a strong release of inflammatory cytokines (IL-1β, IL-6, IL-10 and TNF-α, Fig. 1 A-D) and NO (Fig. 1 E). After adjustment for multiple testing, DOX monotherapy significantly reduced the release of IL-1β ($p<0.002$), IL-6 ($p<0.002$), TNF-α ($p<0.0001$) and NO ($p<0.001$) compared to CRO monotherapy. Accordingly, CRO+DOX significantly decreased IL-6 ($p<0.02$), TNF-α ($p<0.0001$) and NO ($p<0.001$) levels. DAP monotherapy and combination therapy with CRO+DAP reduced the inflammatory reaction to a greater extent with clearly lowered inflammatory cytokines – except IL-10 – (all $p<0.0001$ for CRO vs. DAP and CRO vs. CRO+DAP) and NO release ($p<0.0001$ for all combinations containing DAP). Notably, combined triple therapy with CRO+DOX+DAP significantly decreased the release of IL-1β, IL-6, TNF-α and NO (all $p<0.0001$ for CRO+DOX+DAP vs. CRO) and was the only therapy to significantly reduce IL-10 concentrations compared to CRO monotherapy ($p<0.03$). *S. pneumoniae* exposure did not induce a visible cytopathic effect on astroglial cells in any of the treatment groups, as determined by the observation of intact monolayers (data not shown). Therefore, the reported reduction of NO and cytokine production upon DOX and/or DAP therapy cannot be associated to an increased cell death within these groups.

Improved survival and increased weight gain in infant rats with PM

A total of 156 infant Wistar rats were enrolled for this study. One animal was excluded after unsuccessful infection with no detectable bacterial CSF titer at 18 hpi. All other infected animals were

included after having fulfilled at least one criterion for successful infection (positive bacterial CSF titer > 10^6 cfu/ml, reduced clinical score, weight loss, changes in posture).

Infected rats showed reduced survival compared to uninfected controls (Fig. 2 A). Animals receiving the combination adjuvant therapy, demonstrated a significant better survival compared to infected rats with CRO monotherapy (85.8 % vs. 64.1%, long-rank p=0.0052). Compared to uninfected controls, which constantly gained weight within 42 hours after mock-infection, animals with PM showed only a slight weight increase within the first 18 hours (Fig. 2 B). Thereafter, infected animals treated with CRO monotherapy lost weight (2.81 % weight loss at 42 hpi). This weight loss was reduced with combined adjuvant therapy (0.8% weight gain at 42 hpi), resulting in a significantly higher relative weight gain compared to infected animals with CRO monotherapy (p=0.0022). At all measured time points, uninfected animals gained significantly more weight than their infected counterparts, independent of treatment modality (p<0.0001). Upon infection, clinical scores were reduced and reached a minimum at 24 hpi, whereas uninfected animals did not show any changes in clinical scores at any time point (Fig. 2 C). Clinical scores of infected animals treated with combination adjuvant therapy showed a trend to be higher compared to infected animals receiving CRO monotherapy at 24 hpi (p=0.0884). From 24 hpi on, infected rats started to recover and showed an improvement in clinical scores at 42 hpi, still being significantly lower than those of uninfected control animals (p=0.0015 for CRO and p=0.0053 for CRO+DOX+DAP).

Reduction of inflammatory parameters in CSF *in vivo*

Inflammatory cytokines were measured in the CSF of infected animals before and at 6 and 24 hours after treatment initiation (representing 18, 24 and 42 hpi). Before treatment, cytokine levels were comparable between the two infected groups. Compared to animals treated with CRO monotherapy, IL-1β and IL-10 CSF levels were significantly reduced in rats receiving the combination adjuvant therapy six hours after treatment initiation (p=0.0004 and p=0.0128, Fig. 3 A and C). IL-6 and TNF-α revealed a trend towards reduced CSF levels (p=0.071 and p=0.076, Fig. 3 B and D). Twenty-four hours after therapy start, IL-6 was significantly lower in animals receiving combined adjuvant interventions (p=0.0139, Fig. 3 B). IFN-γ levels were similar between the two groups at all time points

(data not shown). Before therapy initiation, bacterial CSF titers were not different with 1.09 ± 0.71 x 10^8 cfu/ml in the CRO group and 1.15 ± 1.26 x 10^8 cfu/ml in the CRO+DOX+DAP group (p=0.772). Six hours after therapy begin, all animals treated with the combined adjuvant intervention had undetectable bacterial titers (<10^2 ± 0 cfu/ml), whereas half of the animals receiving CRO monotherapy still showed detectable but very low bacterial titers in CSF (3.06 ± 0.89 x 10^2 cfu/ml), representing a significantly faster bacterial clearance in CSF with combined adjuvant therapy (p=0.0236, Fig. 3 E).

Reduced cerebral complication *in vivo*

PM-induced cerebral damage was assessed in all animals sacrificed at 42 hpi. Cortical necrosis was only found in animals with PM. Its extent was significantly higher in the group treated with CRO monotherapy compared to animals receiving combined adjuvant therapy (0.73 % [IQR 0-9.7, n=15] vs. 0% [IQR 0-0, n=15] p=0.0302, Fig. 3 F). Elevated levels of hippocampal apoptosis were only found in infected animals (data not shown). Here, however, no differences between the two treatment groups were found (CRO monotherapy: 0.89 ± 0.91, n=13 vs. CRO+DOX+DAP therapy: 0.92 ± 1.26, n=15 apoptotic cells per visual field, p=0.943).

Improvement of hearing capacity three weeks after infection

To investigate long-term neurologic sequelae induced by PM, hearing capacity was assessed by auditory evoked brainstem response (ABR) three weeks after infection. Representative ABR recordings from a control animal and an infected rat are shown in figure 4 A and B, respectively. Control animals showed detectable responses down to 35 dB, whereas the infected animal did not show any measurable signal below 65dB (Fig. 4 A and B). The average hearing threshold was 38.13 ± 2.39 dB or 38.75 ± 1.44 dB in uninfected animals that received CRO monotherapy or combined adjuvant therapy, respectively (Fig. 4 C). Compared to uninfected rats, infected animals showed significantly higher average hearing thresholds, irrespective of therapy regimen. Treatment with combined adjuvant therapy showed a trend for improved hearing capacity compared to CRO monotherapy (63.26 ± 23.9 dB vs. 72.88 ± 24.8 dB, p=0.0891, Fig. 4 C) in infected rats. In experiments with severely infected animals (defined as an in-litter mortality > 15%), severe hearing

loss (average hearing threshold ≥ 80 dB) was observed, with no difference between therapies. When considering only experiments with an in-litter mortality of less than 15% (mild infection experiments), combination adjuvant therapy with DAP and DOX – compared to CRO monotherapy – significantly reduced PM-induced hearing loss (48.00 ± 21.7 dB, n=10 vs. 67.22 ± 25.9 dB, n=9, p=0.0482).

Univariate linear regression (table 1) analysis revealed significantly increased hearing threshold with increasing bacterial inoculum (70.5 dB per additional log of infection inoculum, p<0.001). Low in-litter mortality and higher clinical score at 24 hpi were both found to predict attenuation of PM-induced hearing impairments (-18.1 dB in case of mildly infected animals, p=0.011; -26.7 dB per additional point of activity score at 24 hpi, p<0.001). Multivariate linear regression modelling (table 1) – including infection inoculum, litter mortality and treatment regimen – displayed comparable findings. After adjusting for in-litter mortality and bacterial inoculum, combination adjuvant therapy was found to significantly reduce PM-induced hearing loss by 10.3 dB (p=0.037).

Improved hearing is associated with reduced fibrous occlusion of the perilymphatic space

To investigate the reason for improved hearing capacity in mildly infected rats treated with combination adjuvant therapy, histomorphological damage in inner ear was assessed by immunofluorescence. Previous work showed that PM-induced hearing loss was accompanied by reduced spiral ganglion neuron density in the cochlea – being a critical predictor for the efficacy of a cochlear implant (25). Spiral ganglion neurons were quantified in the basal, middle and apical turn of mildly-infected animals, as indicated in figure 5 A. No statistical differences were found between the two treatment groups at any of the cochlear turns (fig. 5 C). In the present study, only few animals showed a reduction in SGN density (< 2000 TUJ^+ cells/mm^2, e.g. left middle turn in Fig. 5 A), as compared to SGN density previously reported in mock-infected animals (25). Histomophological assessment of the cochlear turns revealed extensive fibrous occlusion of the perilymphatic space in infected animals (Fig. 5 B). Fibrous occlusion was significantly reduced in infected animals treated with the combined adjuvant intervention compared to animals receiving CRO monotherapy (Fig. 5 D). In mildly-infected animals, a significant positive correlation was found for fibrous occlusion of the perilymphatic space and hearing threshold (Fig. 5 E, r=0.5051, p=0.0274).

Antimicrobial Agents and Chemotherapy

Discussion

Observational clinical studies repetitively found neurologic sequelae in patients surviving bacterial meningitis, with especially high risk after PM (3). A profound inflammatory reaction in the CNS and PNS is associated with cortical necrosis, hippocampal apoptosis and cochlear damage (11–13, 24–26). In addition to bacterial toxins, the host's excessive inflammatory reaction contributes to the observed neural cell death (15–17). Bacterial autolysis and also bactericidal antibiotics with antibiotic-dependent lysis of bacteria provoke a release of highly immunogenic products, promoting inflammatory processes and disease severity (15, 61–64). During PM, secreted MMPs from activated immune cells are crucially upregulated and associated with brain injury (15, 34, 65) with higher MMP-9 level being associated with the development of hearing impairment or secondary epilepsy in infected children (65). By degrading basal lamina components and tight junction proteins, MMP-9 weakens the blood-brain-barrier (BBB) (58, 66–68) and facilitates leukocyte extravasation and BBB leakage (33, 69). Additionally, MMPs contribute to the inflammatory reaction and brain injury via their sheddase and convertase activity, being able to cleave and activate inflammatory cytokines and chemokines (33, 70–72).

DOX has multiple anti-inflammatory effects by reducing cytokine release and inhibiting MMP activity (50–56). Pharmacologic inhibition of MMPs during acute bacterial meningitis resulted in the reduction of blood-brain barrier permeability, inflammatory cytokine levels in CSF, brain injury and mortality (34, 42, 57, 58). Selective MMP inhibitors (e.g. BB-94, BB-1101, GM-6001 or TNF-484) have not yet been successfully tested in clinical studies. DOX, on the other hand, has a well-characterized clinical safety profile (56). The herein used dosage of DOX was previously shown by others to suppress cerebral MMP-9 activity and reduce ischemic brain damage in rodents (73, 74). In experimental infant rat PM, adjuvant DOX reduced mortality and injury to the brain and cochlea (56).

DAP, a non-bacteriolytic but bactericidal antibiotic, integrates itself into the bacterial cell membrane, induces its depolarisation and biosynthesis inhibition (75–77). In previous work, we demonstrated a faster bacterial clearance from CSF with DAP leading to reduced inflammatory parameters and decreased cortical complication compared to standard CRO therapy in infant rat PM (45, 78). In the

same infant rat PM model, adjunctive DAP to CRO reduced PM-associated cerebral damage, inflammatory cytokine levels in the CSF and improved hearing capacity (32, 42). In adult rats with PM, DAP treatment attenuated cognitive impairment in surviving rats compared to CRO (79).

Our previous work on the herein reported experimental model – but also other independent experimental work – confirmed the potential of combined adjuvant interventions targeting multiple pathophysiological mechanisms during PM, thereby improving acute and neurofunctional outcomes (42, 43). With this study, we were able to show that combined adjuvant therapies in experimental paediatric PM cumulate previously reported beneficial effects of single adjuvants and significantly improve acute neuropathology and neuroinflammation, thereby improving neurofunctional outcome compared to standard CRO monotherapy. Combined adjuvant therapy with DAP and DOX was able to improve survival and weight gain in infant rats infected with *S. pneumoniae* (Fig. 2 A, B). Adjuvant DOX – but not DAP – previously demonstrated its capacity to significantly improve survival among infant rats with PM (32, 56). Tetracyclines also demonstrated mortality reduction in experimental sepsis models (80). On the other hand, adjuvant DAP was beforehand shown to improve weight change after treatment initiation (32). Herein, adjuvant combination therapy with DOX and DAP significantly reduced inflammatory cytokines in CSF *in vitro* and *in vivo* (Fig. 1 and 3). Despite previous findings, which showed reduced CSF levels of TNF-α upon DOX-induced TACE inhibition (56) and reduced CSF IL-6 levels with adjuvant DAP (32), we only found statistical trends toward lower CSF levels of these cytokines six hours after treatment initiation (Fig. 3 B,D). Of note, animals treated with combined adjuvant therapy showed slightly higher initial TNF-α and IL-6 levels (18 hpi) with faster subsequent reduction after therapy initiation. In other experimental inflammatory diseases, DOX was shown to inhibit interleukin-converting enzyme, thereby lowering the bioavailability of IL-1β (56, 81). In accordance with this data, we found significantly reduced IL-1β levels six hours after initiating therapy *in vivo* with combined adjuvant intervention compared to CRO monotherapy. Therapy initiation with CRO monotherapy caused increased CSF levels of IL-1β and IL-6, indicating that bacterial burst by lytic antibiotic further aggravates cerebral inflammation (44, 45, 63), which we were able to inhibit with adjuvant non-bacteriolytic DAP *in vitro* and *in vivo*. Our *in vitro* model of neuroinfection and neuroinflammation with primary rat astroglial cells supported the concept of

induced neuroinflammation upon therapy initiation with a bacteriolytic antibiotic with clearly reduced inflammatory cytokines and NO release by treatment with non-bacteriolytic antibiotics (Fig. 1). The reduced induction of neuroinflammation *in vitro* by simultaneous application of CRO+DAP (and CRO+DOX+DAP) underlines previous findings showing fast antibacterial action of DAP (45) and thereby supports the concept of DAP's anti-inflammatory actions even when applied concomitantly with CRO.

Animals receiving combined CRO+DOX+DAP showed significantly reduced cortical damage 42 hpi (Fig. 3 F), without showing a better outcome in terms of hippocampal apoptosis (not shown). The reduced cortical complication might be attributed to the overall reduction of CSF inflammation, as previously found by single adjuvant DAP and DOX therapy (32, 56).

Combined adjuvant therapy with CRO+DOX+DAP improved hearing thresholds in mildly infected infant rats (Fig. 4 D), whereas severely infected animals showed profound hearing loss (average hearing threshold ≥ 80 dB), which might be beyond potential protection. These data were confirmed by a multivariate linear regression showing that after adjusting for infection inoculum and high in-litter mortality, rats with combined adjuvant therapy revealed improved hearing capacity by 10.3 dB (Table 1). Histologic analysis revealed that spiral ganglion neuron density was not significantly affected in mildly infected rats (Fig. 5 C) compared to previously published data of mock-infected infant rats (25). Improved hearing capacity in animals with combined adjuvant therapy was correlated to a significant reduction of fibrous occlusion of the perilymphatic space (Fig. 5 D, E). Fibrous obliteration of the perilymphatic space after experimental PM has been described in a mouse model of PM and positively correlated with increased hearing loss (37). During acute infection, leukocytes enter the perilymphatic space contributing to the inflammatory processes (26). Resolution of the granulocytic inflammation is expected to cause occlusion of the perilymphatic space with connective tissue, potentially leading to cochlear ossification (26). As cochlear ossification can limit the access for cochlear implantations (82), a reduction in fibrous obliteration with associated cochlear ossification has important clinical consequences. Of note, cochlear hair cells and presynaptic ribbons of surviving inner hair cells were not analysed during this study. The detected improvement in hearing

capacity with combined adjuvant DAP and DOX might also be attributed to a protection of cochlear hair cells or their connectivity to the SGNs. In previous work, we demonstrated that connectivity of inner hair cells to SGNs was already reduced after mild infection, whereas the inner hair cells themselves remained unaffected (25). In mildly infected animals with low level fibrotic occlusion, loss of inner hair cell connectivity might explain elevated hearing thresholds (Fig. 5 E).

In a comprehensive meta-analysis, adjunctive anti-inflammatory corticosteroids were shown to improve the outcome of adults with PM in high income countries and children with meningitis caused by *Haemophilus influenzae* type b, without showing a clear benefit of corticosteroids in children with PM (27). Multiple experimental models of bacterial meningitis with adjunctive dexamethasone demonstrated aggravated mortality and acute hippocampal injury with subsequent learning and memory deficits, especially in infant rodents (23, 30, 31, 83, 84). As there is no substantial evidence for the use of dexamethasone in children with PM, we did not include it in our study focussing on paediatric PM. Further limitations of this study include the lack of direct comparison to single adjuvant therapies. As the respective single adjuvant therapies were already tested in our laboratory on the same model of PM, we decided to not include these therapy groups but to compare to previously reported data (32, 56). Additionally, we would like to mention the limitation of direct intracisternal inoculation of pneumococci to induce PM, which does not represent the pathophysiologic route of infection via the bloodstream (15). Yet, development of meningitis after intranasal inoculation with bloodstream spread and hematogenous CNS infection is only obtained is a small proportion of the infected animals – even after experimentally induced extracellular matrix degradation (85) – limiting the use of this inoculation method for specific research on meningitis. Furthermore, animals in our experiments were treated for 5 days and not 10-14 days as recommended for humans (28). Previous experiments showed, however, that this treatment duration resulted in a complete bacterial clearance with associated recovery of clinical scores and weight loss (25, 32, 42). Lastly, resulting CSF daptomycin levels of 0.5mg/L in patients with neurological infections (47, 86) are just slightly above the MIC for *S. pneumoniae* (60) and this may affect the beneficial effects seen in our animal model."

Conclusion

Combination adjuvant therapy with non-bacteriolytic DAP and DOX with its MMP-inhibitory and anti-inflammatory properties caused faster bacterial clearance and reduced inflammatory CSF cytokine levels, known to be mediators of brain damage during acute PM. Previously reported beneficial effects of these single adjuvants were merged together by combined intervention and improved survival, weight loss, cerebral complication and neurologic sequelae such as hearing loss. Therefore, we conclude that combining adjuvant DAP and DOX with CRO is a promising therapeutic option to improve the outcome of PM.

Material and Methods

Infecting organism

A clinical isolate of *Streptococcus pneumoniae* (serotype 3) from a patient with bacterial meningitis was cultured overnight in brain heart infusion (BHI) medium, diluted 10 fold in fresh, pre-warmed BHI medium, and grown for 5 h to reach the logarithmic phase as reported earlier (32, 58). The bacteria were centrifuged for 10 min at 3100 x g, washed twice and re-suspended in sterile, pyrogen-free saline (NaCl 0.85%). Bacteria were further diluted to the desired density by measuring the optical density at 570nm (OD_{570}). Inoculum accuracy was determined by serial dilutions and plating on Columbia sheep blood agar (CSBA) plates.

Antibiotic susceptibility testing

For MIC determination, blood agar plates were inoculated with S. pneumoniae serotype 3 – the strain used within this study. MICs of ceftriaxone (0.002-32mg/L; Liofilchem srl, Italy), doxycycline (0.016-256 mg/L, bioMérieux, USA) and daptomycin (0.016-256 mg/L, bioMérieux, USA) were determined by using antibiotic gradient strips, according to the manufacturer's protocol and as described before (45).

In vitro model of neuroinfection and neuroinflammation

Primary rat astroglial cells, isolated from the cortex and hippocampus of infant rats on post-natal day 3 were kept in culture medium (DMEM [Sigma-Aldrich, Merck Switzerland] with 5% FCS [Biochrom, Germany], GlutaMAX™ [ThermoFisher, Switzerland] and antibiotic-antimycotic [ThermoFisher, Switzerland]) for 11 days at 37°C with 5% CO2, as reported elsewhere (87, 88). For stimulation assays, cells were seeded in poly-L-ornithine-coated 24-well plates and kept for additional 3 days. Subsequently, cell culture medium was replaced with phenol red-free and pyruvate-free DMEM (Gibco, ThermoFisher, Switzerland) with 5% FCS and GlutaMAX™. Cells were stimulated with 3 x 10^7 CFU/mL *S. pneumoniae* in logarithmic growth phase. Directly after stimulation with living bacteria, antibiotics were added to the cell culture medium (10µg/ml CRO [Rocephine, Roche)], 1µg/ml DAP [Cubicin, Cubist Pharmaceuticals], 3µg/ml DOX [doxycycline hyclate, Sigma]),

reflecting CSF concentrations found in patients or experimental studies focusing on neuroinfections (46–49, 86, 89, 90). Nitric oxide production was measured using Griess reagent (Sigma-Aldrich, Merck Switzerland). Briefly, 100 µL Griess reagent was mixed with 100 µL cell culture medium in 96-well plates. Absorbance was measured at 550 nm with a microplate reader (THERMOmax, Molecular Devices, USA). Nitrite concentrations were calculated from a $NaNO_2$ standard curve.

Infant rat model of pneumococcal meningitis

All animal studies were approved by the Animal Care and Experimentation Committee of the Canton of Bern, Switzerland (license BE 129/14), and followed the Swiss national guidelines for the performance of animal experiments. A well-established infant rat model of PM was used for the experiments as previously described (32, 58). Eleven days old Wistar rats together with their dams were obtained from Charles River Laboratories (Sulzfeld, Germany). The dams were provided with tap water and pellet diet at libitum. Litters were kept in rooms at a controlled temperature of 22 ± 2 °C. During the acute phase of the disease, animals were housed in conventional cages in a room with natural light. For long-term experiments after bacterial curing, animals were transferred to individually ventilated cages (IVC) in a room with controlled 12-hour light/dark cycles. Intracisternal infections were performed by injection of 10 µl saline containing 7.33 ± 3.4 x 10^5 cfu/ml living *S. pneumoniae*. Mock-infected control animals received an equivalent volume of saline. Pneumococcal meningitis was confirmed 18 h post infection (hpi) by quantitative analysis of bacterial titers in CSF samples, when the animals developed symptomatic disease. For this, 5 µl of CSF were collected by puncture of the cisterna magna, followed by serial dilution and cultivation on columbia sheep blood agar (CSBA) plates. The infected animals were randomized for treatment with CRO (100mg/kg, Rocephine, Roche, twice daily [b.i.d]) plus: a.) combination adjuvant therapy (n=72) consisting of DAP (10 $mg*kg^{-1}$ d^{-1}, s.c. in saline, single dose; Cubicin, Cubist Pharmaceuticals) plus DOX (30mg/kg, i.p, once daily, Sigma, combined with CRO), or b.) saline in the control group (n=72). Antibiotic therapy with CRO was started at 18 hpi in all animals. Therapies involving DAP were started by the application of DAP followed by a 15 min-delayed application (i.e. at 18:15 hpi) of other therapies. For long-term

experiments assessing neurofunctional outcomes, CRO and DOX therapies were continued until day 5 after infection. Mock-infected animals either received the combination adjuvant therapy (n=6) or the CRO monotherapy with vehicles (n=6). All animals received the same amount of fluids during the experiments.

The rats were weighted and examined clinically at 0, 18, 24 hpi, and before sacrificing at 42 hpi, as previously described (58). Activity scores represent 1 = coma; 2 = does not turn upright; 3 = turns upright within 30 s; 4 = minimal ambulatory activity, turns upright in < 5 s; and 5 = normal. Weight was assessed relative to weight at time of infection (per cent increase). Investigators were blinded for treatment modalities. Spontaneous mortality was documented. Punctures of the cisterna magna were performed using a 30-gauge needle to obtain CSF samples at 18, 24, and 42 hpi. CSF samples not used for bacterial titer determination were centrifuged (16'000 x *g* at 4 °C for 10 min), and the supernatants were frozen at -80 °C until further use. Animals were sacrificed with an overdose of pentobarbital (150 mg/kg b.w., i.p Esconarkon, Streuli Pharma AG, Uznach, Switzerland) at 42 hpi and perfused with ice-cold 4% paraformaldehyde (PFA) in phosphate-buffered saline (PBS) before their brains were removed and fixed in 4 % PFA for histological analysis.

Histomorphometric assessment of cortical damage and hippocampal apoptosis

Damage to cerebral structures was quantified as previously described in all animals sacrificed at 42 hpi (33, 91, 92). Briefly, brains were fixed in 4 % PFA and cryopreserved in 18 % sucrose in PBS at 4 °C overnight. Coronal brain cryosections (45 µm thick) obtained by systematic uniform sampling were stained for Nissl substance with cresyl violet. Cortical damage was defined as areas of decreased neuronal density. Histological features of apoptosis were quantified in 48 systematic visual fields spanning the hippocampus of both hemispheres. Histologic assessments were performed and evaluated by a person blinded to treatment modalities.

Quantitative analysis of cytokine levels in the CSF

A panel of cytokines previously found to be upregulated in PM (15, 93) – i.e. IL-1β, IL-6, TNF-α, IL-10 and IFN-γ – was assessed using a magnetic multiplex assay (Rat Magnetic Luminex® Assay,

R&D Systems, Bio-Techne) and a Bio-Plex 200 station (Bio-Rad Laboratories) as previously described (25, 33). Undiluted cell culture supernatant or five microliters of CSF harvested and centrifuged at 18, 24 and 42 hpi were diluted to a final volume of 50 µl using the provided assay buffer. At least 50 beads were measured for each analyte. Calibration curves from recombinant standards were calculated with Bio-Plex Manager software (version 4.1.1) using a five-parameter logistic curve fitting. For samples below the detection limit, the value of detection limit provided by the manufacturer (TNF-α, 22.1 pg/ml; IL-6, 56.0 pg/ml; IL-1β, 26.7 pg/ml; IL-10, 18.6 pg/ml; IFN-γ, 70.5 pg/ml) was multiplied by the dilution factor.

Click- and pure tone-evoked auditory brainstem response

Auditory brainstem responses (ABRs) were recorded in response to click stimulations and pure tones on both ears using the SmartEP system (Intelligent Hearing Systems, Miami, USA), as previously described (25). Animals were anesthetized with isoflurane (5 % for induction and 2 % for maintenance) using the Combi-Vet Vaporizer System equipped with a digital flowmeter (Rothacher Medical, Switzerland). 100 µs click stimuli and five millisecond pure tone pips (Blackman envelope; polarity alternating) were presented at a rate of 21.1 s^{-1}, ranging from 100 to 20 dB SPL in 10 dB decrements (5 dB decrements close to threshold). A total of 1024 responses were averaged at each sound level and filtered between 100 and 1500 Hz. The hearing threshold was defined as the lowest intensity that induced the appearance of a visually detectable first peak. ABRs were recorded between P30 to P34. Hearing thresholds were independently analysed and discussed by multiple blinded investigators.

Immunohistological analysis of spiral ganglion neuron density and cochlear occlusion

Immunohistological analysis of the cochlea was performed as reported earlier (25). In summary, three weeks after infection, the animals were sacrificed and perfused with 4% paraformaldehyde (PFA). Cochleas were dissected and isolated followed by overnight fixation in 4% PFA at 4°C. Samples were decalcified with Osteosoft (Merck) for 10 d before dehydration and cryopreservation in 30% sucrose followed by cryosectioning. Fourteen µm midmodiolar sections were cut and mounted on Superfrost

Plus microscopy slides (Thermo Fisher Scientific). The immunofluorescence procedure was performed using a Shandon Sequenza staining rack (Thermo Fisher Scientific). Sections were permeabilized for 5 min with 0.1% Triton X-100 and then blocked with a blocking solution (2% BSA plus 0.01% Triton X-100 in PBS) for 1 h at room temperature. The neuron-specific primary antibody against β-III Tubulin (TUJ, mono-clonal mouse anti β-III Tubulin, R&D Systems) was diluted 1:500 in blocking solution and incubated overnight at 4°C. The slides were rinsed three times with PBS and incubated with the secondary antibody (Alexa Fluor 488 conjugated, Invitrogen) diluted 1:500 in blocking solution for 2 h at room temperature. After washing three times with PBS, the samples were mounted with a coverslip using Fluoroshield containing DAPI (Sigma). Images of the spiral ganglion were acquired with a Zeiss Axio Imager M1 with Zeiss EC Plan-Neofluar objectives using AxioVision software (AxioVs40 V 4.8.2.0, Carl Zeiss MicroImagin GmbH).

Statistical analysis

Statistical analyses were performed with GraphPad Prism software (Prism 7 for Windows; GraphPad Software Inc., San Diego, CA). If not stated otherwise, results are presented as mean values ± standard deviations. To compare data between two groups, an unpaired Student t test was used for parametric data. For non-parametric data, a Mann-Whitney test was used. For *in vitro* cytokines and NO release comparing multiple different groups, Tukey's multiple comparison test was applied to adjust for multiple testing. Mortality rates were calculated using log rank (Mantel-Cox) test for significance based on all infected animals and numbers of animals sacrificed for ethical reasons (clinical score of 2) or dying spontaneously. In box-plots, the horizontal line within the box represents the median, the top and bottom of the box mark the 75^{th} and the 25^{th} percentiles, respectively. The upper and lower bound of the whiskers represent the range of the data. A Pearson correlation was performed to correlate cochlear occlusion with hearing capacity. A two-tailed p-value of <0.05 was considered statistically significant, with $p<0.05$ (*), $p<0.01$ (**), $p<0.001$ (***) and $p<0.0001$ (****).

For exploratory data analysis, a multivariate linear regression model was used to estimate predictors and determinants for bacterial meningitis-induced hearing loss. The linear coefficients and a 95%

confidence interval were calculated for each variable. Statistical analyses were performed using STATA 12 (STATA Corp., College Station, TX).

Acknowledgements

We thank Franziska Simon and Robert Lukesch for excellent technical support. Productive discussions and inputs from the ESCMID Study Group for Infectious Diseases of the Brain (ESGIB) were highly appreciated. This work was supported by a grant from the Swiss National Science Foundation (Grant 310030-162583).

Conflict of Interests

The authors declare that there are no conflicts of interest regarding the publication of this paper.

References

1. Koedel U, Scheld WM, Pfister H-W. 2002. Pathogenesis and pathophysiology of pneumococcal meningitis. Lancet Infect Dis 2:721–36.

2. Brouwer MC, Heckenberg SGB, de Gans J, Spanjaard L, Reitsma JB, van de Beek D. 2010. Nationwide implementation of adjunctive dexamethasone therapy for pneumococcal meningitis. Neurology 75:1533–1539.

3. Edmond K, Clark A, Korczak VS, Sanderson C, Griffiths UK, Rudan I. 2010. Global and regional risk of disabling sequelae from bacterial meningitis: a systematic review and meta-analysis. Lancet Infect Dis 10:317–328.

4. Chandran A, Herbert H, Misurski D, Santosham M. 2011. Long-term Sequelae of Childhood Bacterial Meningitis: an underappreciated problem. Pediatr Infect Dis J 30:3–6.

5. Baraff LJ, Lee SI, Schriger DL. 1993. Outcomes of bacterial meningitis in children: a meta-analysis. Pediatr Infect Dis J 12:389–94.

6. van de Beek D, de Gans J, Spanjaard L, Weisfelt M, Reitsma JB, Vermeulen M. 2004. Clinical Features and Prognostic Factors in Adults with Bacterial Meningitis. N Engl J Med 351:1849–1859.

7. McIntyre PB, O'Brien KL, Greenwood B, van de Beek D, Booy R, Heath P. 2012. Effect of vaccines on bacterial meningitis worldwide. Lancet (London, England) 380:1703–11.

8. van de Beek D. 2012. Progress and challenges in bacterial meningitis. Lancet 380:1623–1624.

9. van de Beek D, Farrar JJ, de Gans J, Mai NTH, Molyneux EM, Peltola H, Peto TE, Roine I, Scarborough M, Schultsz C, Thwaites GE, Tuan PQ, Zwinderman A. 2010. Adjunctive dexamethasone in bacterial meningitis: a meta-analysis of individual patient data. Lancet Neurol 9:254–263.

10. Nau R, Soto A, Bruck W. 1999. Apoptosis of Neurons in the Dentate Gyrus in Humans

496 Suffering from Bacterial Meningitis: J Neuropathol Exp Neurol 58:265–274.

497 11. Gerber J, Raivich G, Wellmer A, Noeske C, Kunst T, Werner A, Brück W, Nau R. 2001. A
498 mouse model of Streptococcus pneumoniae meningitis mimicking several features of human
499 disease. Acta Neuropathol 101:499–508.

500 12. Grandgirard D, Steiner O, Täuber MG, Leib SL. 2007. An infant mouse model of brain damage
501 in pneumococcal meningitis. Acta Neuropathol 114:609–617.

502 13. Bifrare Y-D, Gianinazzi C, Imboden H, Leib SL, Täuber MG. 2003. Bacterial meningitis
503 causes two distinct forms of cellular damage in the hippocampal dentate gyrus in infant rats.
504 Hippocampus 13:481–488.

505 14. Grandgirard D, Bifrare Y-D, Pleasure SJ, Kummer J, Leib SL, Täuber MG. 2007.
506 Pneumococcal Meningitis Induces Apoptosis in Recently Postmitotic Immature Neurons in the
507 Dentate Gyrus of Neonatal Rats. Dev Neurosci 29:134–142.

508 15. Mook-Kanamori BB, Geldhoff M, Poll T van der, Beek D van de. 2011. Pathogenesis and
509 Pathophysiology of Pneumococcal Meningitis. Clin Microbiol Rev 24:557–591.

510 16. Mitchell L, Smith SH, Braun JS, Herzog K, Weber JR, Tuomanen EI. 2004. Dual Phases of
511 Apoptosis in Pneumococcal Meningitis. J Infect Dis 190:2039–2046.

512 17. Agyeman P, Grandgirard D, Leib SL. 2014. Chapter 23: Pathogenesis and Pathophysiology of
513 Bacterial Infections., p. . *In* Scheld, MW, Marra, CM, Whitley, RJ (eds.), Infections of the
514 Central Nervous System. Lippincott Williams & Wilkins.

515 18. Iliev AI, Stringaris AK, Nau R, Neumann H. 2003. Neuronal injury mediated via stimulation of
516 microglial toll-like receptor-9 (TLR9). FASEB J 18:412–4.

517 19. Marques CP, Cheeran MC-J, Palmquist JM, Hu S, Lokensgard JR. 2008. Microglia are the
518 major cellular source of inducible nitric oxide synthase during experimental herpes
519 encephalitis. J Neurovirol 14:229–238.

20. Wellmer A, Noeske C, Gerber J, Munzel U, Nau R. 2000. Spatial memory and learning deficits after experimental pneumococcal meningitis in mice. Neurosci Lett 296:137–40.

21. Loeffler JM, Ringer R, Hablützel M, Täuber MG, Leib SL. 2001. The Free Radical Scavenger α-Phenyl-tert-Butyl Nitrone Aggravates Hippocampal Apoptosis and Learning Deficits in Experimental Pneumococcal Meningitis. J Infect Dis 183:247–252.

22. Nau R, Brück W. 2002. Neuronal injury in bacterial meningitis: mechanisms and implications for therapy. Trends Neurosci 25:38–45.

23. Leib SL, Heimgartner C, Bifrare Y-D, Loeffler JM, Täuber MG. 2003. Dexamethasone Aggravates Hippocampal Apoptosis and Learning Deficiency in Pneumococcal Meningitis in Infant Rats. Pediatr Res 54:353–357.

24. Perny M, Solyga M, Grandgirard D, Roccio M, Leib SL, Senn P. 2017. Streptococcus pneumoniae -induced ototoxicity in organ of Corti explant cultures. Hear Res 350:100–109.

25. Perny M, Roccio M, Grandgirard D, Solyga M, Senn P, Leib SL. 2016. The Severity of Infection Determines the Localization of Damage and Extent of Sensorineural Hearing Loss in Experimental Pneumococcal Meningitis. J Neurosci 36:7740–9.

26. Klein M, Koedel U, Pfister H-W, Kastenbauer S. 2003. Morphological Correlates of Acute and Permanent Hearing Loss During Experimental Pneumococcal Meningitis. Brain Pathol 13:123–132.

27. Brouwer MC, McIntyre P, Prasad K, van de Beek D. 2015. Corticosteroids for acute bacterial meningitis, p. CD004405. *In* van de Beek, D (ed.), Cochrane Database of Systematic Reviews. John Wiley & Sons, Ltd, Chichester, UK.

28. van de Beek D, Cabellos C, Dzupova O, Esposito S, Klein M, Kloek AT, Leib SL, Mourvillier B, Ostergaard C, Pagliano P, Pfister HW, Read RC, Sipahi OR, Brouwer MC, ESCMID Study Group for Infections of the Brain (ESGIB). 2016. ESCMID guideline: diagnosis and treatment of acute bacterial meningitis. Clin Microbiol Infect 22:S37–S62.

29. Peltola H, Roine I, Fernandez J, Gonzalez Mata A, Zavala I, Gonzalez Ayala S, Arbo A, Bologna R, Goyo J, Lopez E, Mino G, Dourado de Andrade S, Sarna S, Jauhiainen T. 2010. Hearing Impairment in Childhood Bacterial Meningitis Is Little Relieved by Dexamethasone or Glycerol. Pediatrics 125:e1–e8.

30. Spreer A, Gerber J, Hanssen M, Schindler S, Hermann C, Lange P, Eiffert H, Nau R. 2006. Dexamethasone Increases Hippocampal Neuronal Apoptosis in a Rabbit Model of Escherichia coli Meningitis. Pediatr Res 60:210–215.

31. Coimbra RS, Loquet G, Leib SL. 2007. Limited Efficacy of Adjuvant Therapy with Dexamethasone in Preventing Hearing Loss Due to Experimental Pneumococcal Meningitis in the Infant Rat. Pediatr Res 62:291–294.

32. Grandgirard D, Burri M, Agyeman P, Leib SL. 2012. Adjunctive daptomycin attenuates brain damage and hearing loss more efficiently than rifampin in infant rat pneumococcal meningitis. Antimicrob Agents Chemother 56:4289–4295.

33. Liechti FD, Grandgirard D, Leppert D, Leib SL. 2014. Matrix metalloproteinase inhibition lowers mortality and brain injury in experimental pneumococcal meningitis. Infect Immun 82:1710–8.

34. Leib SL, Clements JM, Lindberg RLP, Heimgartner C, Loeffler JM, Pfister L-A, Täuber MG, Leppert D. 2001. Inhibition of matrix metalloproteinases and tumour necrosis factor α converting enzyme as adjuvant therapy in pneumococcal meningitis. Brain 124:1734–1742.

35. Auer M, Pfister LA, Leppert D, Täuber MG, Leib SL. 2000. Effects of clinically used antioxidants in experimental pneumococcal meningitis. J Infect Dis 182:347–350.

36. Högen T, Demel C, Giese A, Angele B, Pfister H-W, Koedel U, Klein M. 2013. Adjunctive N-acetyl-L-cysteine in treatment of murine pneumococcal meningitis. Antimicrob Agents Chemother 57:4825–30.

37. Klein M, Koedel U, Pfister H-W, Kastenbauer S. 2003. Meningitis-associated hearing loss:

Protection by adjunctive antioxidant therapy. Ann Neurol 54:451–458.

38. Masouris I, Klein M, Dyckhoff S, Angele B, Pfister HW, Koedel U. 2017. Inhibition of DAMP signaling as an effective adjunctive treatment strategy in pneumococcal meningitis. J Neuroinflammation 14:214.

39. Woehrl B, Brouwer MC, Murr C, Heckenberg SGB, Baas F, Pfister HW, Zwinderman AH, Morgan BP, Barnum SR, van der Ende A, Koedel U, van de Beek D. 2011. Complement component 5 contributes to poor disease outcome in humans and mice with pneumococcal meningitis. J Clin Invest 121:3943–53.

40. Mook-Kanamori BB, Rouse MS, Kang C-I, van de Beek D, Steckelberg JM, Patel R. 2009. Daptomycin in experimental murine pneumococcal meningitis. BMC Infect Dis 9:50.

41. Kasanmoentalib ES, Valls Seron M, Morgan BP, Brouwer MC, van de Beek D. 2015. Adjuvant treatment with dexamethasone plus anti-C5 antibodies improves outcome of experimental pneumococcal meningitis: a randomized controlled trial. J Neuroinflammation 12:149.

42. Muri L, Grandgirard D, Buri M, Perny M, Leib SL. 2018. Combined effect of non-bacteriolytic antibiotic and inhibition of matrix metalloproteinases prevents brain injury and preserves learning, memory and hearing function in experimental paediatric pneumococcal meningitis. J Neuroinflammation 15:233.

43. Klein M, Höhne C, Angele B, Högen T, Pfister HW, Tüfekci H, Koedel U. 2018. Adjuvant non-bacteriolytic and anti-inflammatory combination therapy in pneumococcal meningitis: an investigation in a mouse model. Clin Microbiol Infect.

44. Stucki A, Cottagnoud M, Winkelmann V, Schaffner T, Cottagnoud P. 2007. Daptomycin Produces an Enhanced Bactericidal Activity Compared to Ceftriaxone, Measured by [3H]Choline Release in the Cerebrospinal Fluid, in Experimental Meningitis Due to a Penicillin-Resistant Pneumococcal Strain without Lysing Its Cell Wall. Antimicrob Agents

595 Chemother 51:2249–2252.

596 45. Grandgirard D, Schürch C, Cottagnoud P, Leib SL. 2007. Prevention of brain injury by the
597 nonbacteriolytic antibiotic daptomycin in experimental pneumococcal meningitis. Antimicrob
598 Agents Chemother 51:2173–8.

599 46. Gerber P, Stucki A, Acosta F, Cottagnoud M, Cottagnoud P. 2006. Daptomycin is more
600 efficacious than vancomycin against a methicillin-susceptible Staphylococcus aureus in
601 experimental meningitis. J Antimicrob Chemother 57:720–723.

602 47. Kullar R, Chin JN, Edwards DJ, Parker D, Coplin WM, Rybak MJ. 2011. Pharmacokinetics of
603 single-dose daptomycin in patients with suspected or confirmed neurological infections.
604 Antimicrob Agents Chemother 55:3505–9.

605 48. Cottagnoud P, Pfister M, Acosta F, Cottagnoud M, Flatz L, Kuhn F, Muller H-P, Stucki A.
606 2004. Daptomycin Is Highly Efficacious against Penicillin-Resistant and Penicillin- and
607 Quinolone-Resistant Pneumococci in Experimental Meningitis. Antimicrob Agents Chemother
608 48:3928–3933.

609 49. Yim CW, Flynn NM, Fitzgerald FT. 1985. Penetration of oral doxycycline into the
610 cerebrospinal fluid of patients with latent or neurosyphilis. Antimicrob Agents Chemother
611 28:347–8.

612 50. Brown DL, Desai KK, Vakili BA, Nouneh C, Lee H-M, Golub LM. 2004. Clinical and
613 Biochemical Results of the Metalloproteinase Inhibition with Subantimicrobial Doses of
614 Doxycycline to Prevent Acute Coronary Syndromes (MIDAS) Pilot Trial. Arterioscler Thromb
615 Vasc Biol 24:733–738.

616 51. Roach D., Fitridge R., Laws P., Millard S., Varelias A, Cowled P. 2002. Up-regulation of
617 MMP-2 and MMP-9 Leads to Degradation of Type IV Collagen During Skeletal Muscle
618 Reperfusion Injury; Protection by the MMP Inhibitor, Doxycycline. Eur J Vasc Endovasc Surg
619 23:260–269.

620 52. Golub LM, Lee H-M, Ryan ME, Giannobile WV, Payne J, Sorsa T. 1998. Tetracyclines Inhibit
621 Connective Tissue Breakdown by Multiple Non-Antimicrobial Mechanisms. Adv Dent Res
622 12:12–26.

623 53. Pasquale TR, Tan JS. 2005. Nonantimicrobial Effects of Antibacterial Agents. Clin Infect Dis
624 40:127–135.

625 54. Gabler WL, Creamer HR. 1991. Suppression of human neutrophil functions by tetracyclines. J
626 Periodontal Res 26:52–8.

627 55. Suomalainen K, Sorsa T, Golub LM, Ramamurthy N, Lee HM, Uitto VJ, Saari H, Konttinen
628 YT. 1992. Specificity of the anticollagenase action of tetracyclines: relevance to their anti-
629 inflammatory potential. Antimicrob Agents Chemother 36:227–9.

630 56. Meli DN, Coimbra RS, Erhart DG, Loquet G, Bellac CL, Täuber MG, Neumann U, Leib SL.
631 2006. Doxycycline Reduces Mortality and Injury to the Brain and Cochlea in Experimental
632 Pneumococcal Meningitis. Infect Immun 74:3890–3896.

633 57. Paul R, Lorenzl S, Koedel U, Sporer B, Vogel U, Frosch M, Pfister H-W. 1998. Matrix
634 metalloproteinases contribute to the blood-brain barrier disruption during bacterial meningitis.
635 Ann Neurol 44:592–600.

636 58. Leib SL, Leppert D, Clements J, Täuber MG. 2000. Matrix metalloproteinases contribute to
637 brain damage in experimental pneumococcal meningitis. Infect Immun 68:615–20.

638 59. The European Committee on Antimicrobial Susceptibility Testing. 2019. Breakpoint tables for
639 interpretation of MICs and zone diameters, version 9.0.

640 60. Pankuch GA, Jacobs MR, Appelbaum PC. 2003. Bactericidal activity of daptomycin against
641 Streptococcus pneumoniae compared with eight other antimicrobials. J Antimicrob Chemother
642 51:443–6.

643 61. Tomasz A, Moreillon P, Pozzi G. 1988. Insertional inactivation of the major autolysin gene of
644 Streptococcus pneumoniae. J Bacteriol 170:5931–4.

645 62. Tuomanen E, Liu H, Hengstler B, Zak O, Tomasz A. 1985. The induction of meningeal
646 inflammation by components of the pneumococcal cell wall. J Infect Dis 151:859–68.

647 63. Nau R, Eiffert H. 2005. Minimizing the release of proinflammatory and toxic bacterial products
648 within the host: A promising approach to improve outcome in life-threatening infections.
649 FEMS Immunol Med Microbiol 44:1–16.

650 64. Nau R, Eiffert H. 2002. Modulation of release of proinflammatory bacterial compounds by
651 antibacterials: potential impact on course of inflammation and outcome in sepsis and
652 meningitis. Clin Microbiol Rev 15:95–110.

653 65. Leppert D, Leib SL, Grygar C, Miller KM, Schaad UB, Hollander GA. 2000. Matrix
654 Metalloproteinase (MMP)-8 and MMP-9 in Cerebrospinal Fluid during Bacterial Meningitis:
655 Association with Blood-Brain Barrier Damage and Neurological Sequelae. Clin Infect Dis
656 31:80–84.

657 66. Rosenberg GA. 2002. Matrix metalloproteinases in neuroinflammation. Glia 39:279–291.

658 67. Yang Y, Estrada EY, Thompson JF, Liu W, Rosenberg GA. 2007. Matrix Metalloproteinase-
659 Mediated Disruption of Tight Junction Proteins in Cerebral Vessels is Reversed by Synthetic
660 Matrix Metalloproteinase Inhibitor in Focal Ischemia in Rat. J Cereb Blood Flow Metab
661 27:697–709.

662 68. McColl BW, Rothwell NJ, Allan SM. 2008. Systemic Inflammation Alters the Kinetics of
663 Cerebrovascular Tight Junction Disruption after Experimental Stroke in Mice. J Neurosci
664 28:9451–9462.

665 69. Sellner J, Leib SL. 2006. In bacterial meningitis cortical brain damage is associated with
666 changes in parenchymal MMP-9/TIMP-1 ratio and increased collagen type IV degradation.
667 Neurobiol Dis 21:647–656.

668 70. Leppert D, Lindberg RLP, Kappos L, Leib SL. 2001. Matrix metalloproteinases:
669 multifunctional effectors of inflammation in multiple sclerosis and bacterial meningitis. Brain

Res Rev 36:249–257.

71. Khokha R, Murthy A, Weiss A. 2013. Metalloproteinases and their natural inhibitors in inflammation and immunity. Nat Rev Immunol 13:649–665.

72. Song J, Wu C, Zhang X, Sorokin LM. 2013. In Vivo Processing of CXCL5 (LIX) by Matrix Metalloproteinase (MMP)-2 and MMP-9 Promotes Early Neutrophil Recruitment in IL-1 - Induced Peritonitis. J Immunol 190:401–410.

73. Lee CZ, Xu B, Hashimoto T, McCulloch CE, Yang G-Y, Young WL. 2004. Doxycycline Suppresses Cerebral Matrix Metalloproteinase-9 and Angiogenesis Induced by Focal Hyperstimulation of Vascular Endothelial Growth Factor in a Mouse Model. Stroke 35:1715–1719.

74. Clark WM, Lessov N, Lauten JD, Hazel K. 1997. Doxycycline treatment reduces ischemic brain damage in transient middle cerebral artery occlusion in the rat. J Mol Neurosci 9:103–108.

75. Steenbergen JN, Alder J, Thorne GM, Tally FP. 2005. Daptomycin: a lipopeptide antibiotic for the treatment of serious Gram-positive infections. J Antimicrob Chemother 55:283–288.

76. Sauermann R, Rothenburger M, Graninger W, Joukhadar C. 2008. Daptomycin: A Review 4 Years after First Approval. Pharmacology 81:79–91.

77. Baltz RH. 2009. Daptomycin: mechanisms of action and resistance, and biosynthetic engineering. Curr Opin Chem Biol 13:144–151.

78. Grandgirard D, Oberson K, Bühlmann A, Gäumann R, Leib SL. 2010. Attenuation of cerebrospinal fluid inflammation by the nonbacteriolytic antibiotic daptomycin versus that by ceftriaxone in experimental pneumococcal meningitis. Antimicrob Agents Chemother 54:1323–1326.

79. Barichello T, Gonçalves JCN, Generoso JS, Milioli GL, Silvestre C, Costa CS, Coelho J da R, Comim CM, Quevedo J. 2013. Attenuation of cognitive impairment by the nonbacteriolytic

695 antibiotic daptomycin in Wistar rats submitted to pneumococcal meningitis. BMC Neurosci
696 14:42.

697 80. Maitra SR, Bhaduri S, Valane PD, Tervahartiala T, Sorsa T, Ramamurthy N. 2003. Inhibition
698 of matrix metalloproteinases by chemically modified tetracyclines in sepsis. Shock 20:280–5.

699 81. Solomon A, Rosenblatt M, Li DQ, Liu Z, Monroy D, Ji Z, Lokeshwar BL, Pflugfelder SC.
700 2000. Doxycycline inhibition of interleukin-1 in the corneal epithelium. Invest Ophthalmol Vis
701 Sci 41:2544–57.

702 82. Senn P, Rostetter C, Arnold A, Kompis M, Vischer M, Häusler R, Ozdoba C, Mantokoudis G,
703 Caversaccio M. 2012. Retrograde cochlear implantation in postmeningitic basal turn
704 ossification. Laryngoscope 122:2043–2050.

705 83. Bally L, Grandgirard D, Leib SL. 2016. Inhibition of Hippocampal Regeneration by Adjuvant
706 Dexamethasone in Experimental Infant Rat Pneumococcal Meningitis. Antimicrob Agents
707 Chemother 60:1841–6.

708 84. Zysk G, Brück W, Gerber J, Brück Y, Prange HW, Nau R. 1996. Anti-inflammatory treatment
709 influences neuronal apoptotic cell death in the dentate gyrus in experimental pneumococcal
710 meningitis. J Neuropathol Exp Neurol 55:722–8.

711 85. Zwijnenburg PJG, van der Poll T, Florquin S, van Deventer SJH, Roord JJ, van Furth AM.
712 2001. Experimental Pneumococcal Meningitis in Mice: A Model of Intranasal Infection. J
713 Infect Dis 183:1143–1146.

714 86. Piva S, Di Paolo A, Galeotti L, Ceccherini F, Cordoni F, Signorini L, Togni T, De Nicolò A,
715 Rasulo FA, Fagoni N, Latronico N, D'Avolio A. 2019. Daptomycin Plasma and CSF Levels in
716 Patients with Healthcare-Associated Meningitis. Neurocrit Care.

717 87. Hupp S, Heimeroth V, Wippel C, Förtsch C, Ma J, Mitchell TJ, Iliev AI. 2012. Astrocytic
718 tissue remodeling by the meningitis neurotoxin pneumolysin facilitates pathogen tissue
719 penetration and produces interstitial brain edema. Glia 60:137–146.

720 88. Iliev AI, Stringaris AK, Nau R, Neumann H. 2004. Neuronal injury mediated via stimulation of
721 microglial toll-like receptor-9 (TLR9). FASEB J 18:412–414.

722 89. Klugman KP, Friedland IR, Bradley JS. 1995. Bactericidal activity against cephalosporin-
723 resistant Streptococcus pneumoniae in cerebrospinal fluid of children with acute bacterial
724 meningitis. Antimicrob Agents Chemother 39:1988–1992.

725 90. Karlsson M, Hammers S, Nilsson-Ehle I, Malmborg AS, Wretlind B. 1996. Concentrations of
726 doxycycline and penicillin G in sera and cerebrospinal fluid of patients treated for
727 neuroborreliosis. Antimicrob Agents Chemother 40:1104–7.

728 91. Gianinazzi C, Grandgirard D, Imboden H, Egger L, Meli DN, Bifrare Y-D, Joss PC, Täuber
729 MG, Borner C, Leib SL. 2003. Caspase-3 mediates hippocampal apoptosis in pneumococcal
730 meningitis. Acta Neuropathol 105:499–507.

731 92. Gehre F, Leib SL, Grandgirard D, Kummer J, Bhlmann A, Simon F, Gumann R, Kharat AS,
732 Tuber MG, Tomasz A. 2008. Essential role of choline for pneumococcal virulence in an
733 experimental model of meningitis. J Intern Med 264:143–154.

734 93. van Furth AM, Roord JJ, van Furth R. 1996. Roles of proinflammatory and anti-inflammatory
735 cytokines in pathophysiology of bacterial meningitis and effect of adjunctive therapy. Infect
736 Immun 64:4883–90.

737

738

Figure legends

Fig. 1 Inflammatory cytokines and nitric oxide (NO) production upon *in vitro* stimulation of astroglial cells with living *S. pneumoniae*. Cytokines and NO were measured in cell culture supernatant 24 hours after concomitant application of living *S. pneumoniae* and antibiotics. Infection and bacteriolysis induced by ceftriaxone (CRO) resulted in high levels of IL-1β (**A**), IL-6 (**B**), TNF-α (**D**) and NO (**F**) release, whereas no clear effect was found for IFN-γ (**E**). All therapies containing non-bacteriolytic antibiotics significantly reduced the release of inflammatory cytokines compared to CRO monotherapy (all $p<0.01$ for CRO vs. DOX; $p<0.001$ for CRO vs. CRO+DOX, CRO vs. DAP, CRO vs. CRO+DAP; $p<0.0001$ for CRO vs. CRO+DOX+DAP). Doxycycline (DOX) monotherapy and all combination therapies containing daptomycin (DAP) significantly reduced NO production compared to CRO monotherapy (all $p<0.0001$). Significance levels are not indicated in the graphs for clearer representation. Statistical differences were assessed using unpaired t-tests.

753 **Fig.2 Clinical data of infant rats during acute pneumococcal meningitis.** Combined antibiotic
754 therapy (n=72) with daptomycin (DAP), doxycycline (DOX) and ceftriaxone (CRO) significantly
755 improved survival compared to CRO monotherapy (n=71) during acute PM (**A**). Relative weight
756 change during acute PM indicates reduced weight gain in infected (PM+) compared to mock-infected
757 (PM-) animals (n=6 per treatment group). Infected animals with combined adjuvant therapy presented
758 significantly increased weight change at 42 hpi, compared to CRO monotherapy (**B**). Clinical scoring
759 revealed reduced clinical scores in all infected compared to mock-infected animals (**C**). Differences
760 were assessed by an unpaired t-test in (B) and (C) and with a Log-rank test to compare survival in A.

761 **Fig. 3 Inflammatory CSF cytokine levels, cortical necrosis and bacterial clearance from CSF**
762 **during the acute PM.** Cytokine levels are represented by mean ± 95% confidence interval starting
763 before treatment initiation, 6 hours and 24 hours after treatment start (representing 18, 24 and 42 hpi)
764 for IL-1β (**A**), IL-6 (**B**), IL-10 (**C**) and TNF-α (**D**). Combination adjuvant therapy (n=11) significantly
765 reduced IL-1β, IL-6 and IL-10 CSF levels compared to CRO monotherapy (n=11), while showing a
766 trend towards reduced TNF-α CSF level 6 hours after treatment start. Bacterial titers in the CSF were
767 similar in both treatment groups before starting therapy (at 18 hpi; n=53 for CRO/DAP/DOX, n=49 for
768 CRO) with a faster bacterial clearance in animals receiving the combined adjuvant therapy (n=17)
769 compared to CRO monotherapy (n=18, **E**). Cortical necrosis was only found in animals with PM and
770 was significantly reduced by combined adjuvant therapy (n=15) compared to CRO monotherapy
771 (n=15, **F**). Statistical differences were assessed using an unpaired t-test for cytokines and bacterial titer
772 at 18 hpi. For necrotic cortex volume and bacterial titer at 24 hpi a Mann-Whitney test was used as
773 data were not normally distributed.

774

Fig. 4 Hearing capacity assessed three weeks after acute pneumococcal meningitis. Representative ABR recordings from a mock-infected rat (**A**) with a hearing threshold of 35dB compared to an infected rat (**B**) with an elevated hearing threshold of 65dB. Perceived sound intensities are indicated with dashed lines. Infected animals receiving combined adjuvant therapy (n=25) showed a trend towards improved hearing thresholds compared to animals receiving CRO monotherapy (n=23, **C**). Combined adjuvant therapy significantly reduced hearing loss in mildly infected animals (n=10) compared to CRO monotherapy (n=9, **D**).

Fig. 5 Immunohistological analysis of spiral ganglion neuron density and cochlear occlusion in mildly infected animals. (**A**) Midmodiolar section showing the basal (B), middle (M) and apical (A) turns of an infected rat three weeks after PM immunostained for neurons (β-III tubulin, green) and cell nuclei (DAPI, blue). The absence and presence of fibrous occlusion in the perilymphatic space in a mock-infected control animal and in an infected animal receiving standard CRO monotherapy is represented in over-exposed immunofluorescence pictures (**B**). The area with fibrous occlusion in the perilymphatic space is indicated by white dashed lines. Spiral ganglion neuron (SGN) density was not significantly different in any of the cochlear turns in infected animals between the two treatment groups (**C**). Combined adjuvant therapy (n=10) significantly reduced the amount of fibrous tissue in the perilymphatic space compared to CRO monotherapy (n=9, **D**). A significant positive correlation for fibrous occlusion of the perilymphatic space and hearing threshold was found (**E**).

Antimicrobial Agents and Chemotherapy

796 ## Table with legend

797 **Table 1.** Univariate and multivariate linear regression for click hearing thresholds three weeks after
798 surviving an episode of acute pneumococcal meningitis (n=48).

Hearing Thresholds						
	Univariate			Multivariate		
	Coef.	95% CI	p	Coef.	95% CI	p
Bacterial inoculum (per add. log)	70.5	45.6-95.5	<0.001	69.9	48.2-91.6	<0.001
Comb. Adjuv. Therapy	-9.7	-23.8-4.4	0.172	-10.3	-19.9- -0.6	0.037
Low in-litter mortality	-18.1	-31.8- -4.3	0.011	-17.1	-26.9- -7.3	0.001
Activity @ 24hpi (per add. score)	-26.7	-39.5- -14.02	<0.001	-	-	-

799

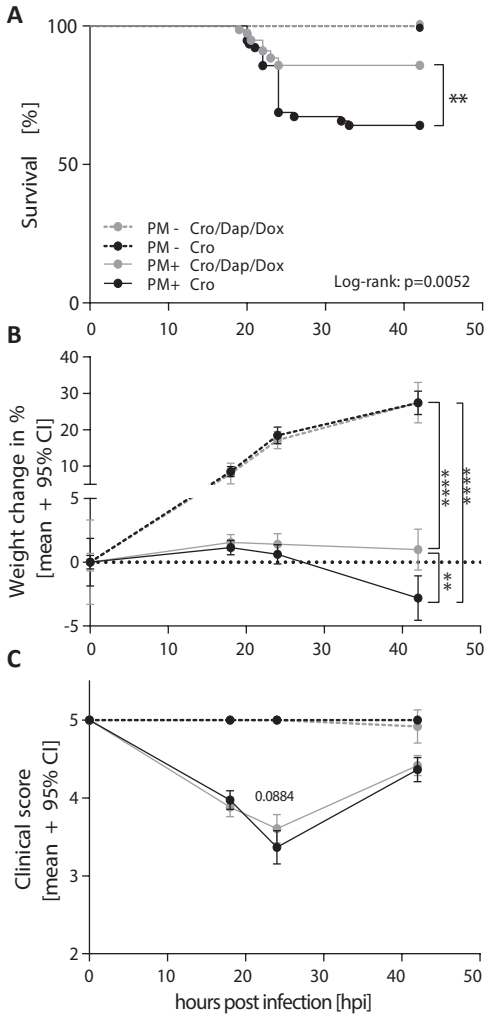

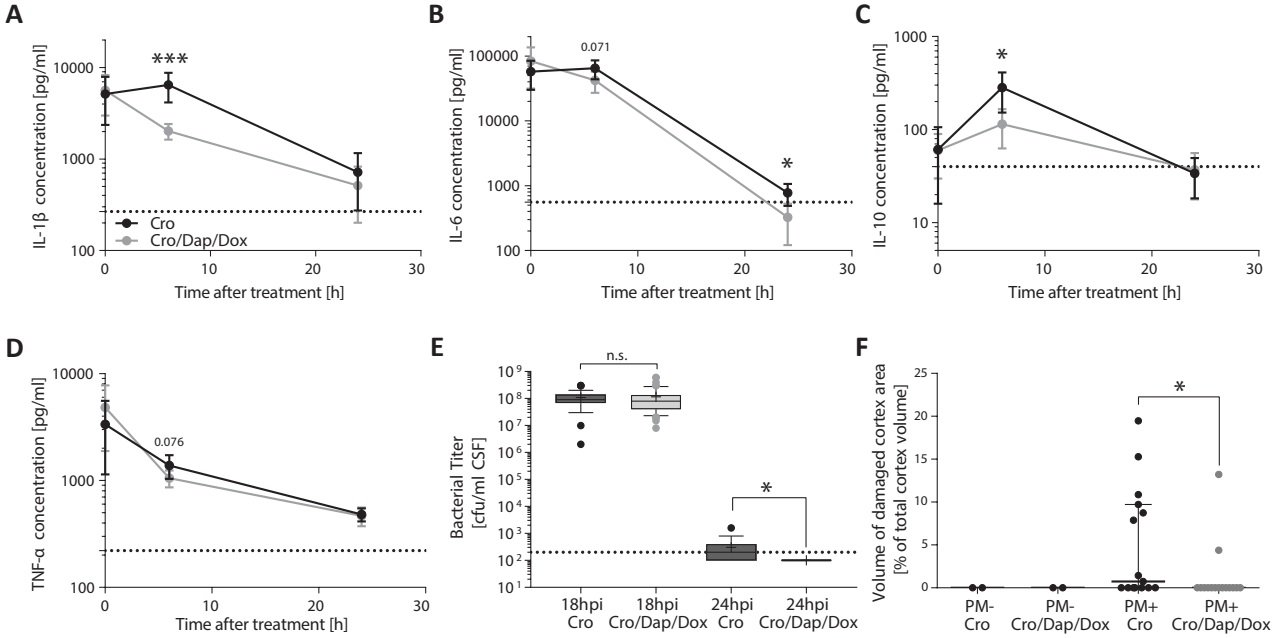

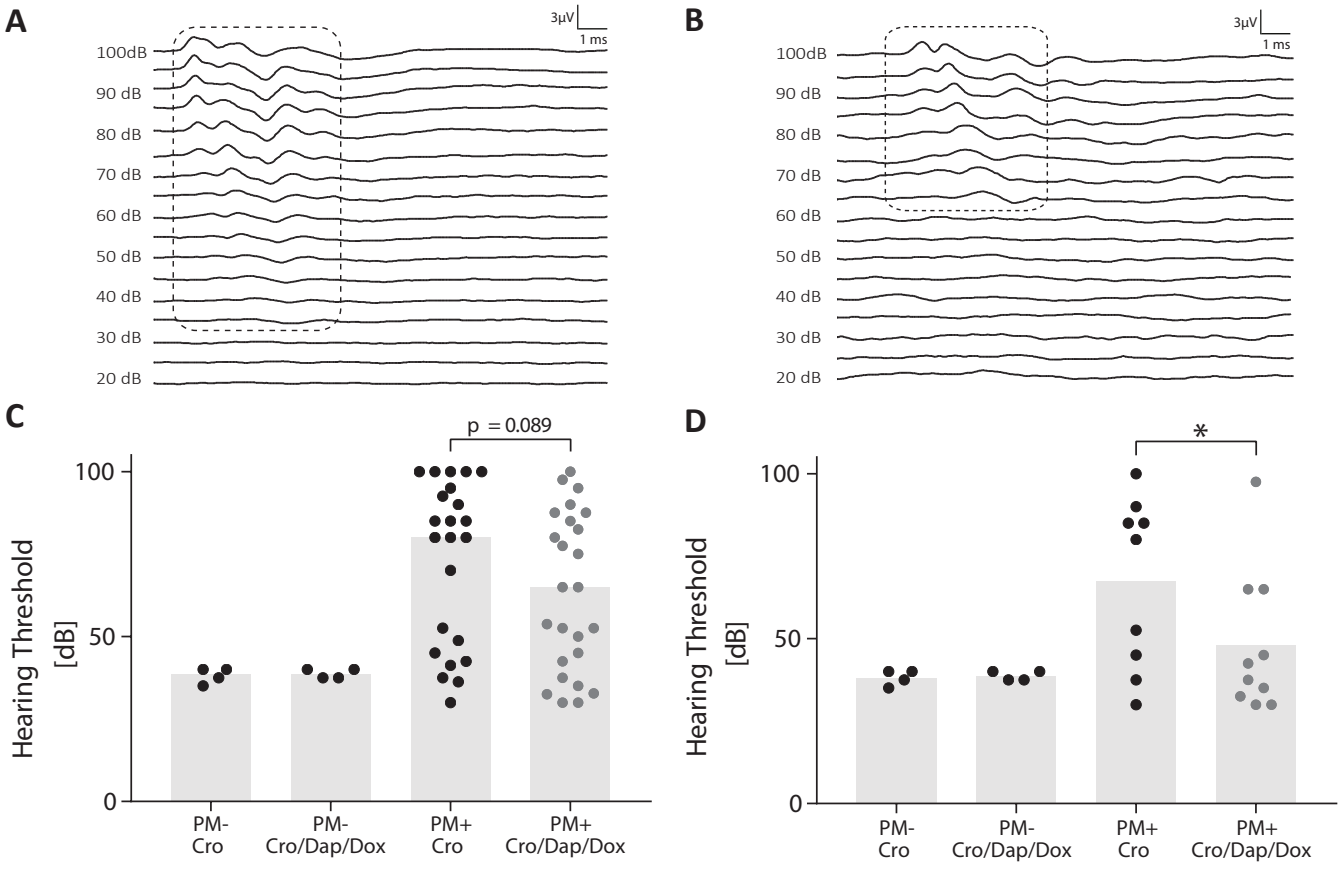

Antimicrobial Agents and Chemotherapy